Geminate recombination in protontransfer reactions. IV. Groundstate yields

Noam Agmon

Citation: The Journal of Chemical Physics **89**, 1524 (1988); doi: 10.1063/1.455149
View online: http://dx.doi.org/10.1063/1.455149
View Table of Contents: http://scitation.aip.org/content/aip/journal/jcp/89/3?ver=pdfcov
Published by the AIP Publishing

Geminate recombination in proton–transfer reactions. IV. Ground-state yields

Noam Agmon[a)]
Department of Physical Chemistry, The Hebrew University, Jerusalem 91904, Israel

(Received 29 May 1987; accepted 27 April 1988)

Our calculations of proton–anion distance distribution functions for HPTS dissociation recombination in the excited state are extended to the nanosecond time regime. When these functions are used for averaging the ground-state recombination probability, good agreement with experimental ground-state recombination yields is obtained. The relation with the theory of "delayed" geminate recombination is briefly discussed.

I. INTRODUCTION

In excited-state proton–transfer reactions,[1] a model system which has been extensively studied[2–8] is proton dissociation and recombination from 8-hydroxypyrene 1,3,6-trisulfonate (HPTS). In previous work,[8] we have analyzed in detail the transient kinetics in this system using the Debye–Smoluchoswki equation (DSE) with "backreaction" boundary conditions (BC).[9] In this analysis, the "intrinsic" dissociation and recombination rate constants at contact, κ_d^* and κ_r^*, have been determined. (Ref. 8 lists other relevant experimental parameters for this system). This enables one to extrapolate the numerical calculation of the excited-state diffusional dynamics to long times with good accuracy.

The present work considers the fate of the separated ion pair after the (radiational) decay to the ground state, as depicted in the following scheme:

$$\begin{array}{ccccc} \mathrm{ROH}^* & \rightleftharpoons & \mathrm{RO}^{-*}\cdots\mathrm{H}^+ & & \\ h\nu \uparrow & & \vdots\ h\nu & & \\ \mathrm{ROH} & \xleftarrow[\text{recom.}]{} & \mathrm{RO}^-\cdots\mathrm{H}^+ & \xrightarrow[\text{escape}]{} & \mathrm{RO}^- + \mathrm{H}^+ \end{array} \qquad (1)$$

ROH denotes the triply charged HPTS with its OH group intact, RO^- is its quadruply charged anion, and an asterisk denotes the excited S_1 state.

While the very small pK^* value (~ 1.4) of the excited-state results in almost complete dissociation, the much larger pK value (7.7 ± 0.1) for the ground state means that a considerable fraction of the dissociated ion pairs may recombine in the ground state rather than escape. The recombination probability is larger for pairs which have not separated too much while in the excited state. Hence the average ground-state ultimate recombination probability η is expected to be larger for a shorter radiational lifetime τ of the excited state. This has indeed been observed in a nanosecond experiment,[5] where the dependence of η on τ was determined in two independent measurements. This lifetime τ, which is determined from the decay of the RO^{-*} fluorescence to be 5.5–6.0 ns in pure water,[2,5] diminishes upon addition of the quencher $Hg(CN)_2$. The "ultimate" fraction of recombined molecules η was determined from the absorbance of the ground-state anion (by measuring also at basic conditions, one can calibrate to 100% RO^-). This was done 20 ns after photolysis, a time long enough for the ground-state geminate kinetics to reach its asymptotic limit, but sufficienctly short to prevent complications due to homogeneous recombination.

Since the parameters determining the excited-state diffusional dynamics are now available from our previous work,[8] and the ultimate recombination probability in a Coulomb field from any initial separation r_0 is analytically known,[10–13] one may predict the outcome of the foremention experiments[5] with no adjustable parameters. The procedure for doing so is discussed in Sec. II. Details of the calculation and an estimate of its accuracy are given in Sec. III. It is more accurate and reliable than a previous attempt[6] (see Appendix A). Finally, Sec. IV demonstrates the quantitative agreement obtained between experiment[5] and theory.

II. THEORY

Let us consider the diffusional dynamics of the dissociated proton in the excited and ground states, scheme (1). Quantities of the excited state are denoted here by asterisks. For the excited state we[8] are able to calculate the probability distribution, $p^*(r,t)$, for the proton and RO^{-*} anion to be separated to a distance r at time t after the laser excitation, when no deexcitation mechanism operates. The spatial integral of p^* is the survival probability $Q^*(t)$ of the excited-state geminate pair, while $1 - Q^*(t)$ is the probability of observing a nondissociated ROH^*; $Q^*(t) \equiv \int_a^\infty p^*(r,t) r^2\, dr$, with $a = 6.5$ Å being the "contact distance."[8] The finite radiative lifetime of both excited-state species, $\tau = 5.5$–6.0 ns, is accounted for by multiplying the above by $\exp(-t/\tau)$. The determination of $p^*(r,t)$ from the transient DSE with the appropriate backreaction BC,[9] and the values of the parameters for fitting the picosecond fluorescence decay of ROH^* are presented in the first part of this series.[8(a)]

To calculate the ultimate ($t \to \infty$) ground-state yield[14] of recombined ROH molecules, consider the distribution function for excited-state pairs with a finite lifetime τ, which is given by $p^*(r,t)\exp(-t/\tau)$. Assume that at $t = 0$ the concentration of ground-state ROH molecules is zero, $p(r,0) = 0$. Between t and $t + dt$ the ground-state distribution for RO^- with a proton at r, is reinforced by an infinitesimal decay from the excited state

$$\delta p(r,t) = p^*(r,t) \exp(-t/\tau) dt/\tau. \qquad (2)$$

It is assumed, of course, that there is no change in r during

[a)] Address until August 1988: NIH, DCRT, Bld. 12A Rm. 2007, Bethesda, MD 20892.

 0021-9606/88/151524-05$02.10

the fast electronic transition. The symbol δ is used to indicate that Eq. (2) does not represent the *total* change in the ground-state population $dp(r,t)$.

A pair that has decayed to the ground state when its separation was r has a recombination probability which is denoted by $\eta^0(r)$. This quantity is known analytically (Appendix B).[12] The observed ground-state escape probability $1-\eta$ is obtained by averaging $1-\eta^0(r)$ with respect to $\delta p(r,t)$ and integrating over time

$$1-\eta = 4\pi\tau^{-1}\int_0^\infty dt \exp(-t/\tau) \times \int_a^\infty dr\, r^2 p^*(r,t)[1-\eta^0(r)] = 4\pi\tau^{-1}\int_a^\infty \bar{p}^*(r,\tau^{-1})[1-\eta^0(r)]r^2\,dr. \quad (3)$$

Here $\bar{p}(r,s)$ is the temporal Laplace transform of $p(r,t)$. This integral, written for the escape probability $1-\eta$, rather than for the reaction probability η, correctly takes into account the fact that ROH* molecules which have not dissociated decay directly to ROH. Note also that Eq. (3) is a special case of Eq. (3) in Ref. 13.

For $\eta^0 = 0$ the integral in Eq. (3) gives the total RO^{-}* population that has decayed radiatively to the ground state up to $t=\infty$ (the absolute RO^{-}* fluorescence quantum yield). The ROH* absolute fluorescence yield is accordingly

$$\phi(\mathrm{ROH}^*) = \tau^{-1}\int_0^\infty [1-Q^*(t)]\exp(-t/\tau)dt. \quad (4)$$

Eventually all population decays radiatively to the ground state, so the two yields must normalize to unity. This could be used as a check for the accuracy of the numerical procedure namely, the sum of $\exp(-t/\tau)r^2p^*(r,t)\Delta r$ over all grid points (including that representing the recombined state) and all times should be unity.

In the present experimental situation the initial distribution is concentrated in the recombined state (i.e., at $t=0$ one has only ROH*). For the case where the initial distribution is a delta function at $r_0>a$, i.e., $4\pi r_0^2 p^*(r,0|r_0)=\delta(r-r_0)$, one may easily obtain an ordinary differential equation for η as a function of r_0. This is done by operating on Eq. (3) with $\mathbf{L}_0^\dagger$, which is the adjoint diffusion operator in initial conditions. Using the well-known (e.g., Ref. 12) "backward equation" for $\bar{p}^*(r,s|r_0)$:

$$\mathbf{L}_0^\dagger \bar{p}^*(r,s|r_0) \equiv D r_0^{-2} e^{-R_D/r_0}\frac{\partial}{\partial r_0} r_0^2 e^{R_D/r_0}\frac{\partial}{\partial r_0}\bar{p}^* = s\bar{p}^* - (4\pi r_0^2)^{-1}\delta(r-r_0) \quad (5)$$

[D is the diffusion constant and R_D the Debye length, determining the extent of the attractive Coulomb potential $V(r) = -R_D/r$], one obtains

$$\tau\,\mathbf{L}_0^\dagger \eta(r_0) = \eta(r_0) - \eta^0(r_0). \quad (6)$$

This result is idential with Eq. (19) in the theory of delayed geminate recombination,[13] obtained there by more complicated manipulations.

III. CALCULATION PROCEDURE AND ACCURACY

The scatter in the experiment results[5] is almost 10% (i.e., ± 0.05). Hence it suffices to perform the calculation to an accuracy of 1%–2%. In this section we give the details of the calculation and evaluate the errors involved. The basic strategy is to solve the DSE for $p^*(r,t)$ using the numerical procedure described in part I,[8(a)] then integrate numerically according to Eq. (3), with $\eta^0(r)$ given in Appendix B. It is first assumed that the ground-state recombination is diffusion controlled, then a small experimentally determined correction factor (Appendix B) is applied in the final quantitative comparison.

The parameters for propagating the DSE at 23-25 °C are[8] $D = 950$ Å^2/ns, $R_D = 28.5$ Å, and $a = 6.5$ Å. These are slightly different than those used in Ref. 6, but the differences are negligible: Decreasing D to 900 Å^2/ns results in an increase of $\sim 0.5\%$ in η, while decreasing R_D to 28 Å leads to a 1% decrease of η. The value of the contact radius a is that recommended in the literature.[4,8] If decreased to 5.5 Å, η increases by 2%.

The value for R_D reflects the Coulomb attraction between the proton and the quadruply charged RO^{-}*. The potential used does not include corrections for the ionic strength, which is $\sim 1\times 10^{-4}$ M, and is due mainly to the dissolved trisodium HPTS salt, whose concentration was[5] 2×10^{-5} M. One can evaluate the error in using the bare (unscreened) Coulomb potential as follows. The largest error is expected for the longest lifetime (6 ns), when protons diffuse far enough to feel the interaction with the sodium ions. At 6 ns, $1/e = 0.37$ of the excited-state population survives. About 40% of this population has the proton at distances larger than that of the nearest Na^+, ~ 180 Å (see Fig. 1). At 180 Å, η^0 (Appendix B) is 0.15 for no screening and 0.04 for complete screening. Hence the error in η is approximately $0.37\times 0.4\times(0.15-0.04) = 0.015$, less than 2% in the most unfavorable condition.

Results are compared for two different boundary conditions (BC) at the contact radius a:

(i) The accurate calculation implies backreaction BC[9] with rate parameters determined from a fit to the picosecond experiments[8] at room temperature. Here $\kappa_d^* = 9.2$ ns^{-1} and $\kappa_r^* = 9$ Å/ns. (These values are subject to errors of at least 10%.) The initial condition was a delta function at the first grid point, which represents the trap at $r<a$.

(ii) The approximate calculation uses a reflecting BC as in Ref. 6, namely $\kappa_d^* = \kappa_r^* = 0$ (see Appendix A). The initial conditions were changed to a delta function concentrated at the *second* grid point. This represents a geminate pair at contact, $r=a$.

The numerical integration was performed to $t_{\max} = 20$ ns with a time step of 20 ps (compared with 0.2 ps in Ref. 6, see Appendix A. This is due to the more accurate Chebyshev propagation scheme[8(a)]). The grid size was 1 Å, and its range 6.5–766 Å. By 20 ns no more than 0.2% of the population has collected at the outer boundary. (For this purpose the outer boundary is absorbing.) Decreasing the time step to 10 ps and/or the grid size to 0.7 Å made a negligible difference (typically less than 0.5%). Note that for $\tau = 6$ ns at $t = 20$ ns almost 4% of the population is still in the excited

state. These geminate pairs, however, have diffused to such large separations that when they eventually decay to the ground state, they mostly separate rather than recombine. To check this point, results for $\tau = 6$ ns were obtained by integration up to 10 and 16 ns. For $t_{max} = 10$ ns, η is smaller by 0.02, while for 16 ns the result is already the same as for integration up to 20 ns.

The above procedure assumes that τ is the same for ROH* and RO^-*. The experimental paper[5] suggests that the radiative decay of ROH* is unaffected by addition of the quencher. The acid, however, dissociates in the excited state within a few tenths of a nanosecond,[7,8] while τ is in the range of 1.5–5.4 ns. By that time there is very little ROH* left, so that its exact lifetime should be of little effect. In fact, it is surprising that it could be measured accurately, when the signal has mostly disappeared. Also, the ROH* peak in the steady-state fluorescence spectrum is only 5% of the total intensity, so that changes in its amplitude following quencher addition would be difficult to detect.

To check the possible abovementioned effect, a term $-p^*(r,t)/\tau$ has been added to the DSE with τ(ROH*) = 6 ns and $\tau(RO^-*)$ varying. The exponential term in Eq. (3) was accordingly deleted. For the smallest value of $\tau(RO^-*) = 1.5$ ns, η was found to decrease by only 0.03.

IV. RESULTS

The temporal evolution of the distribution function $p^*(r,t)$ for the two BCs is compared in Fig. 1. The more accurate calculation with a backreaction BC is shown as a full line. It is seen that the distribution for a reflecting boundary (dashed curve) has diffused further away at any given instant. This is physically clear, since the backreaction BC, which represents recombination with secondary dissociation of the excited-state acid, has introduced a delay in the mutual diffusion process. This delay, which is a few tenths of a nanosecond, becomes negligible on the nanosecond time scale, so that for long times the two distributions converge. Hence we expect the difference in η for the two BCs to diminish as τ increases.

That this is indeed so can be seen in Fig. 2: There is always more recombination for the delayed backreaction

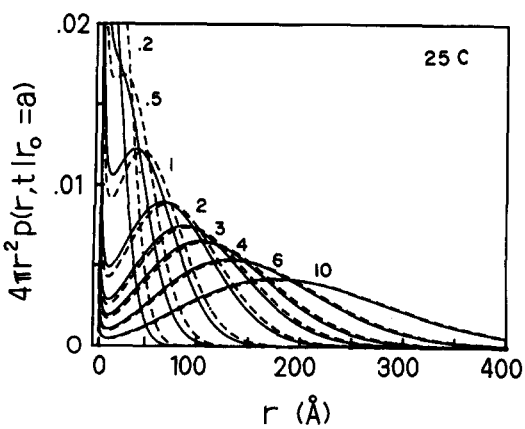

FIG. 1. Temporal evolution of the distribution function, obtained as a numerical solution of the DSE, for the two different boundary conditions: Full line is for reversible recombination dissociation in the excited state (backreaction BC), while the dashed curve is for a nonreactive excited state (reflecting BC). Time (in nanoseconds) labels the curves.

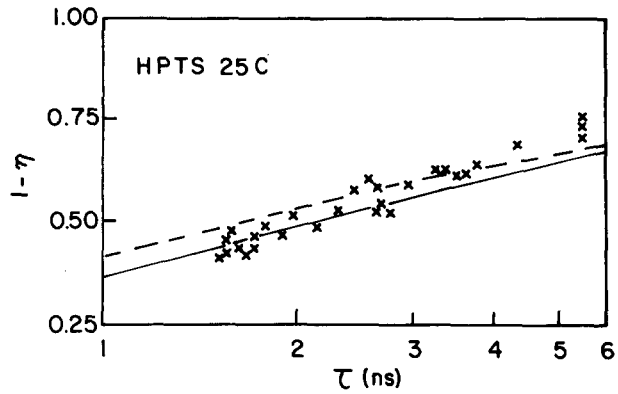

FIG. 2. Ultimate proton escape probability from photodissociated 8-hydroxypyrene 1,3,6-trisulfonate (HPTS) as a function of the radiative lifetime in the excited state. Crosses are experimental results (Ref. 5); full line is the calculation with backreaction BC in the excited state; dashed curve is a similar calculation for a nonreactive excited state (reflecting BC). Both calculations assume absorbing BCs for the ground state.

case, but the two results converge at large τ. The calculation shown is for an absorbing BC for the ground-state recombination process ($\kappa_r = \infty$, see Appendix B). In order to ease comparison with Ref. 5, the scale is the same as in Fig. 5 there. The experimental points (crosses) for no $Hg(CN)_2$ quencher are those on the extreme right, whereas points on the left are for large quencher concentrations. The logarithmic time scale biases the region of small τ, but has no other theoretic justification. A more natural representation is as a function of $\tau^{-1/2}$ (see Appendix C).

Figure 3 shows η as a function of $\tau^{-1/2}$. The experimental results with their estimated error bars are shown as the hatched area. Note that the zero-quencher case is now on the extreme left. The calculation with an absorbing BC for ground-state recombination (line *a*) is corrected for the large but finite ground-state recombination rate, by multiplying it by the ratio of the observed to diffusion-controlled recombination rates (Appendix B)

$$k_{on}/k_D = 0.93 \pm 0.03.$$

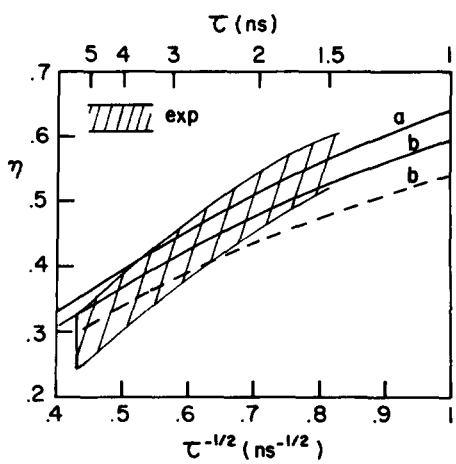

FIG. 3. Ultimate recombination probability in geminate photodissociation of HPTS: A different representation of the data of Fig. 2. Experiment (Ref. 5) with estimated error bars is shown as a hatched area. Full and dashed curves are calculated, with the same two excited-state boundary conditions as in Fig. 2. Line labeled *a* is the same as the full curve in Fig. 2, while lines *b* are the results of Fig. 2 multiplied by $k_{on}/k_D = 0.93$, to account for the finite recombination rate in the ground state.

This factor was taken from Ref. 4. The error bars are certainly an underestimate, since they reflect those in the measurement[4] of k_{on}, and do not include the uncertainties in the diffusion-controlled rate constant (i.e., errors in determining D and R_D).

The final results are therefore lines b in Fig. 3. For the backreaction BC the (full) line passes in between the error bars for the whole range of measured lifetimes. (For the largest τ these results may be too large by 0.02, due to the neglect of screening by the ionic atmosphere.) The result for a reflecting boundary (dashed curve) lies partially outside the error bars. It is not surprising that the largest deviation is for short times, where the difference between the two distributions is not yet negligible (Fig. 1). For a quantitative comparison with experiment at high quencher concentrations one needs to know the exact excited-state diffusional dynamics, as determined from our picosecond fluorescence measurements.[8]

V. CONCLUSION

The nanosecond measurements[5] of the ultimate ground-state recombination yields of photochemically excited HPTS can be explained quantitatively, with no free parameters whatsoever: All required rate parameters were obtained from a fit to the picosecond dissociation experiments in the excited state[8] and the determination of the ground-state recombination rate.[4] These abovementioned sets of experiments, together with the steady-state results discussed in Ref. 8, are the first comprehensive demonstration for the applicability of the continuous Smoluchowski equation as a description of the transient behavior in fast proton–transfer reactions.

It may be interesting to repeat the experiments:

(i) with a shorter laser pulse: The 18 ns pulse used[5] may be too wide compared with the 20 ns delay in measuring the RO^- absorption, and perhaps not all the population has reached its ultimate fate;

(ii) with time-dependent absorption monitoring of the RO^- anion, that could be compared with the temporal evoluation of the geminate pairs in the ground state.

ACKNOWLEDGMENTS

I thank D. Huppert, Dr. R. Kosloff, and Professor E. Pines for discussions.

APPENDIX A

The experimental results[5] have been previously analyzed via the DSE approach in Ref. 6. In this Appendix we compare the two calculations.

In Ref. 6 it was assumed that the excited state is nonreactive (there is no recombination of protons with RO^{-*}) while the ground state is very reactive. The DSE was solved for a Coulomb potential and BCs at the contact radius a which are reflective up to time τ_i and absorbing thereafter (τ_i can be thought as the time when the anion decays to its ground state). The results of the calculation were finally averaged with respect to τ_i [see Eq. (3)]. A quantitative fit to experiment[5] could be obtained only for R_D or a which were different from their experimentally accepted values.

In the light of the recent results of Ref. 8, it is clear that several inadequate assumptions and numerical procedures have been used in Ref. 6:

(i) The excited RO^{-*} is certainly very reactive, as demonstrated by the long time tail in the survival probability measured in the picosecond experiments.[7,8] However the distribution functions for zero recombination (reflecting BC) and fast recombination dissociation (backreaction BC) do converge at long times (see Fig. 1). Therefore, the approximation of Ref. 6, although physically unrealistic, can give qualitatively good results for the recombination yields for long excited-state lifetimes. For a quantitative analysis at high quencher concentrations, the experimentally determined[8] values of κ_d^* and κ_r^* should be used.

(ii) There is no need to continue the integration for the ground-state species namely, for $t > \tau_i$. The escape (vs reaction) probability for a geminate pair in a Coulomb potential is well known (Appendix B) and should be averaged with respect to the excited-state diffusional dynamics as in Eq. (3).

(iii) In the numerical method of finite differences as used in Ref. 6, the largest possible time step was 0.2 ps. Hence the diffusion equation could not be integrated for more than 3 ns, and an extrapolation procedure had to be used. We now have at our disposal[8] a propagation scheme for the DSE, where the integration time step can be taken 100 times larger than that of the simple finite-differencing method. It is therefore possible to propagate to long times (> 20 ns) with good accuracy.

It is likely that a combination of the above three reasons did not allow the previous investigators[5,6] to obtain the quantitative agreement between experiment and theory demonstrated in the present work.

APPENDIX B

For completeness, we cite the expression[12] for the ultimate recombination probability in a Coulomb potential, $V(r) = -R_D/r$, from an initial separation r and a radiation BC (with an intrinsic rate constant κ_r) at $r = a$:

$$\eta^0(r) = [1 - \exp(-R_D/r)]/[1 - \exp(-R_D/a)] + DR_D \exp(-R_D/a)/a^2\kappa_r]. \quad \text{(B1)}$$

Because the denominator does not depend on r, changing κ_r is equivalent to mulitplying the reaction probability for an absorbing boundary ($\kappa_r = \infty$)

$$\eta^0_{\text{abs}}(r) = [1 - \exp(-R_D/r)]/[1 - \exp(-R_D/a)] \quad \text{(B2)}$$

by a constant. Indeed, it is easy to show[15] that [see also Appendix B of Ref. 8(b)]

$$\eta^0(r) = \eta^0_{\text{abs}}(r) k_{on}/k_D. \quad \text{(B3)}$$

k_{on} is the overall steady-state association rate coefficient, while k_D is its upper limit namely, the diffusion-controlled rate constant

$$k_D = 4\pi DR_D/[1 - \exp(-R_D/a)]. \quad \text{(B4)}$$

In the present calculation, η^0_{abs} is used for the integration in Eq. (3), and the result is subsequently multiplied by k_{on}/k_D.

APPENDIX C

The exact solution of the diffusion equation is complicated. It is helpful to develop approximations which give some intuitive feeling to the physics, while still representing the gross overall behavior. A hierarchy of such approximations is presented below.

In the first approximation one can assume that RO^{-*} decays to its ground electronic state exactly at $t=\tau$. Since the average of an exponential distribution in t is $\langle t\rangle=\tau$, this amounts to replacing the time average of p^* in Eq. (3) by its value for the average time τ:

$$\eta\approx 4\pi\int_a^\infty \eta^0(r)p^*(r,\tau)r^2\,dr. \tag{C1}$$

In writing Eq. (C1) it was also assumed that the remaining fraction of ROH* at $t=\tau$ is negligible, so that $p^*(r,\tau)$ normalizes to unity.

As a second approximation let us change the order of spatial averaging, writing $\eta=\eta^0(\langle r\rangle)$, where $\langle r\rangle$ is the average distance with respect to the excited-state probability density function p^* at time τ. By further approximating η^0 by $\eta^0_{\rm abs}$, replacing the denominator in Eq. (B2) by unity (this is Onsager's result,[10] valid when $a\ll R_D$), and expanding the exponent to first order, one finds

$$\eta\approx R_D/\langle r\rangle. \tag{C2}$$

Finally, the simplest approximation is obtained by assuming that

$$\langle r\rangle^2\approx\tfrac{1}{2}\langle r^2\rangle\approx 3D\tau \tag{C3}$$

(the second equality is rigorous for free diffusion, $R_D=0$). Insertion in Eq. (C2) gives

$$\eta\approx R_D/(3D\tau)^{1/2}. \tag{C4}$$

Hence in the crudest approximation η is linear in $\tau^{-1/2}$.

A comparison with experiment of the different approximations is shown in Fig. 4. The approximation of Eq. (C1) is shown as a bold line. It underestimates the exact results by 10%–15%. This is due to the fact that a larger fraction of the excited-state population decays at $t<\tau$ than at $t>\tau$. In addition, at short times the distribution is tightly concentrated near $r=a$, hence contributes more to the reaction probability.

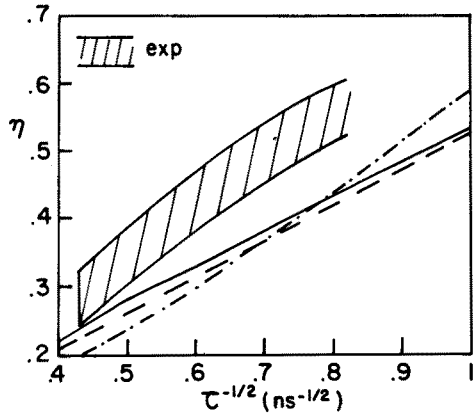

FIG. 4. Comparison of the ultimate recombination probability of HPTS with various approximations: Full curve is Eq. (C1), dash–dotted curve is Eq. (C2), and the dashed line is Eq. (C4).

The approximations of Eqs. (C2) and (C4) are also shown in Fig. 4. They do not differ very much from each other. These approximations, and in particular the simple analytic result given in Eq. (C4), can serve as rough estimates to the exact reaction probability.

[1]E. M. Kosower and D. Huppert, Annu. Rev. Phys. Chem. **37**, 127 (1986).
[2]A. Weller, Z. Phys. Chem. **17**, 224 (1958).
[3]K. Breitschwerdt and A. Weller, Z. Phys. Chem. **20**, 353 (1959).
[4]Th. Förster and S. Völker, Chem. Phys. Lett. **34**, 1 (1975).
[5]M. Hauser, H.-P. Haar, and U. K. A. Klein, Ber. Bunsenges. Phys. Chem. **81**, 27 (1977).
[6]H.-P. Haar, U. K. A. Klein, and M. Hauser, Chem. Phys. Lett. **58**, 525 (1978).
[7]E. Pines and D. Huppert, Chem. Phys. Lett. **126**, 88 (1986); J. Chem. Phys. **84**, 3576 (1986).
[8](a) E. Pines, D. Huppert, and N. Agmon, J. Chem. Phys. **88**, 5620 (1988), first paper in this series; (b) N. Agmon, E. Pines, and D. Huppert, *ibid.* **88**, 5631 (1988), second paper in this series.
[9]F. C. Goodrich, J. Chem. Phys. **22**, 588 (1954); D. L. Weaver, *ibid.* **72**, 3483 (1980); N. Agmon, *ibid.* **81**, 2811 (1984).
[10]L. Onsager, Phys. Rev. **54**, 554 (1938).
[11]K. M. Hong and J. Noolandi, J. Chem. Phys. **68**, 5163 (1978).
[12]H. Sano and M. Tachiya, J. Chem. Phys. **71**, 1276 (1979).
[13]M. Tachiya, Chem. Phys. Lett. **127**, 462 (1986).
[14]N. Agmon, J. Chem. Phys. **82**, 2056 (1985).
[15]D. Shoup and A. Szabo, Biophys. J. **40**, 33 (1982).